

## Energetic charged-particle spectrum following $\mu^-$ capture by nuclei

K. S. Krane, T. C. Sharma, and L. W. Swenson

*Department of Physics, Oregon State University, Corvallis, Oregon 97331*

D. K. McDaniels, P. Varghese, and B. E. Wood

*Department of Physics, University of Oregon, Eugene, Oregon 97403*

R. R. Silbar and H. D. Wohlfahrt

*Los Alamos Scientific Laboratory, Los Alamos, New Mexico 87545*

C. A. Goulding

*Department of Physics, Florida A & M University, Tallahassee, Florida 32307*

(Received 29 May 1979)

The energy spectra of charged particles (mainly protons) emitted following muon capture have been measured for targets of Al, Cu, and Pb. The intensity of the energetic (40–70 MeV) emitted particles falls exponentially with increasing energy,  $I = I_0 \exp(-E/E_0)$ , with exponential constant  $E_0$   $7.5 \pm 0.4$  MeV (Al),  $8.3 \pm 0.5$  MeV (Cu),  $9.9 \pm 1.1$  MeV (Pb). The integrated yield for particles above 40 MeV was found to be  $(1.38 \pm 0.09) \times 10^{-3}$  per capture for Al,  $(1.96 \pm 0.12) \times 10^{-3}$  per capture for Cu, and  $(0.171 \pm 0.028) \times 10^{-3}$  per capture for Pb.

[NUCLEAR REACTIONS Al, Cu, Pb ( $\mu^-, x$ ),  $E = 0$ , measured charged particle spectrum,  $\sigma(E)$ .]

### I. INTRODUCTION

Although neutron emission following nuclear muon capture is a well-studied phenomenon,<sup>1</sup> there is considerably less information available on the number and character of charged particles emitted.<sup>2</sup> The emission of charged particles following nuclear muon capture was first observed by Morinaga and Fry<sup>3</sup> with nuclear emulsions; their results were interpreted by Ishii<sup>4</sup> in terms of statistical emission following compound nuclear formation. This model failed by an order of magnitude to reproduce the observed intensity of proton emission. A more successful account of the proton emission probability was obtained from a calculation done by Singer.<sup>5</sup> In this model, capture takes place on a correlated proton-proton pair ("pseudo-deuteron") at the nuclear surface, and the internal motion then gives rise to the energetic emitted particles. Other theoretical explanations have suggested the presence of structure in the particle spectrum owing to muon interactions with virtual exchange pions<sup>6</sup> and to collective excited states in the daughter nucleus.<sup>7</sup> On the other hand, a structureless spectrum has been predicted by Bernabéu, Ericson, and Jarlskog,<sup>8</sup> using a partially conserved axial vector current (PCAC) argument to relate inclusive  $\mu$  capture with large excitations to pion absorption; they suggest that in 1% of capture

events a high-energy nucleon is emitted. A nuclear emulsion experiment by Kotelchuck and Tyler<sup>9</sup> failed to reveal any such structure; a similar conclusion was derived from a novel experiment by Sobottka and Wills,<sup>10</sup> in which a silicon detector served both as target and particle detector. High-energy protons following muon capture in nuclear emulsions were studied also by Vaisenberg *et al.*<sup>11</sup>

We report here a measurement of the spectrum of charged particles emitted following  $\mu^-$  capture. A previous experiment of the present type was done by Budyashov *et al.*,<sup>12</sup> who observed proton and deuteron emission from several targets. Although their statistics were limited, especially in the upper energy range ( $E > 40$  MeV), their results suggest the emission of larger numbers of high-energy particles than expected from evaporation processes alone. These results were extended to additional nuclei by Balandin *et al.*<sup>13</sup> From these experiments one further concludes that protons comprise the major component of the charged particles.

An estimate of the overall probability for charged-particle emission, relative to neutron emission, can be obtained from the recent activation experiments reported by Wyttenbach *et al.*<sup>14</sup> whose results suggest that the relative charged-particle-emission probability is of order 1% in medium-weight nuclei and falls to 0.1% in heavy

nuclei. An analysis of these results by Lifshitz and Singer<sup>15</sup> was successful in accounting for the observed particle-emission probabilities, in terms of a model which considered both pre-equilibrium and compound-nucleus emission. The former dominates in heavy nuclei, in which the Coulomb barrier inhibits charged-particle emission.

Whatever the correct theoretical interpretation of this phenomenon may be, two features of this experiment must be emphasized: (1) Since the prototype capture reaction ( $\mu^- p \rightarrow \nu n$ ) gives an outgoing neutron, the observation of emitted protons requires a two-step or correlated process. (2) Since capture by a free proton gives a 5-MeV outgoing neutron, the high-energy emitted particles must arise from capture by high-momentum nucleons. Thus a careful measurement of the high-energy particle spectrum can perhaps serve as a sensitive probe of the high-momentum components of the nuclear wave function<sup>16</sup> and possibly of the nucleon-nucleon correlations.

We have therefore undertaken a series of experiments to measure the high-energy spectra of charged particles following nuclear muon capture. In the present work we report on the gross shape of the charged-particle spectrum in the range  $E > 40$  MeV; our results suggest that the spectrum is structureless and decreases exponentially with increasing particle energy. The integrated intensities (above 40 MeV) deduced from our results reveal two puzzling features: (1) The Pb target yields an intensity roughly an order of magnitude smaller than the Al and Cu targets. (2) Compared with the previous data of Budyashov *et al.*,<sup>12</sup> our results show a factor of 2–3 greater intensity with the Cu target. In subsequent work we will report on the relative intensities of the various components of the particle spectrum, and will extend these measurements to other targets in the hope of resolving these two puzzles.

## II. EXPERIMENTAL DETAILS

The experimental arrangement is indicated schematically in Fig. 1. The stopped muon channel at the Los Alamos Meson Physics Facility (LAMPF) was used as a source of 80 MeV/ $c$  muons. A polyethylene moderator of thickness 4 cm was used to slow the beam in order to maximize the number of stops in the target. A standard 2-counter telescope was used to record the muons; a third counter placed behind the target and operated in anticoincidence with the first two counters identified muons which stopped in the target.

Protons were counted using 4 scintillation detectors, each 15 cm by 60 cm and 15 cm thick, arranged into a 60 cm by 60 cm array. A veto count-

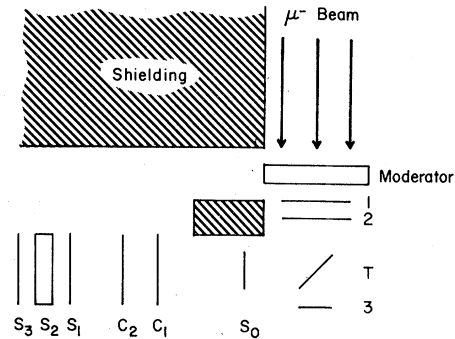


FIG. 1. Schematic diagram of experimental arrangement. Components are represented as follows: 1, 2, 3—muon telescope (logic 123);  $T$ —target;  $S_i$ —particle scintillators ( $S_1$ — $\Delta E$  counter,  $S_2$ —60 cm by 60 cm scintillator array,  $S_3$ —veto counter);  $C_i$ —multiwire proportional chamber.

er served to eliminate particles which did not stop in the scintillator. Thin  $\Delta E$  counters were used in an effort to do particle identification, but owing to the large background present, the effort was not particularly successful. In an attempt to reduce the background and identify those events which came from the target, two multiwire proportional chambers (MWPC's) were used in the later stages of the experiment, but only a limited quantity of data was accumulated in this configuration. An additional thin counter ( $S_0$  in Fig. 1) was added in order to reduce background and define the target more clearly. The effective solid angle of the counting system was about 2% of  $4\pi$ .

Three targets were used in the present experiment: aluminum, copper, and lead metal foils in natural isotopic abundances. Target dimensions were 23 cm by 18 cm. The targets were oriented at 45° to the beam, so that the effective area presented to the beam was 23 cm by 12.5 cm. Target thicknesses were 343 mg/cm<sup>2</sup> (Al), 310 mg/cm<sup>2</sup> (Cu), and 490 mg/cm<sup>2</sup> (Pb).

Data were processed using conventional logic circuitry and written event-by-event onto magnetic tape using a PDP-11 computer through a CAMAC interface. The  $\mu$ -stop logic signal was stretched to compensate for the delayed emission of particles following capture, the delay arising from the lifetime of the muon in the 1s atomic state. Typical gate widths were 100–500 nsec. With the primary LAMPF proton current at 300  $\mu$ A, the instantaneous muon rate was 10<sup>6</sup>/sec, and the stopping rate in our targets was of order 10<sup>4</sup>/sec. Under these circumstances, a one-hour data run yielded the order of 100 events in a 2-MeV bin at 40 MeV.

A particular problem in this experiment was the

large background rate, arising in part from neutrons and high-energy gamma rays emitted in the target and from high-energy electrons and photons associated with the beam. Although the steps taken to reduce background were partially successful, the background rate was still unacceptably high. Even though adding additional detectors, with additional coincidence requirements, effects some reduction in the background, introducing additional detectors into a sea of neutrons and gamma rays results in secondary events which add to the background. Rather than try to identify the source of the background and correct for it, we measured beam-associated background events by physically removing the target; background events resulting from neutrons produced in the target were measured by introducing a 1-cm lead absorber between the target and  $S_0$ , thereby removing all target-associated charged particles. For each target, we thus have three runs: target in and target out without the absorber, and target in with the absorber. The difference between the accumulated histograms of the first two runs gives the events associated with the target, and the third run compared with the first gives the fraction of target events associated with charged particles. Typically, removal of the target reduced the data rate by half, suggesting that half of the observed intensity is associated with the target. Insertion of the lead absorber reduced the rates by about 75%, so that the overall signal-to-noise ratio is of order 1:2.

Calibration of the scintillation detectors was done with the direct muon beam, using relative light output curves to generate the proton calibration points. It is estimated that this procedure yields an energy calibration accurate to within a few tenths of MeV.

### III. RESULTS

As described above, for each target we obtained three histograms, in order to measure beam-induced and target-induced background events. These histograms were normalized by the relative muon rates ("singles" rates of counter 1 or 2 of the muon telescope), which amounted to at most a few per cent variation. The resultant histograms of the particle scintillation detectors were then added. Corrections were applied for energy loss in air and in the thin scintillators in the proton counter system, such corrections amounting to a few MeV. Corrections for energy loss in the target were estimated by assuming that the particle traveled, on the average, half the thickness of the target; this correction was 1–2 MeV over the range of proton energies reported here. Finally the observed muon

stopping rate was used to normalize the ordinates, and the muon stopping rate was converted into a muon capture rate using the ratio of the muon capture rate to the total muon disappearance rate<sup>17</sup> (0.61 for Al, 0.93 for Cu, 0.97 for Pb). The resulting spectra are displayed in Figs. 2–4, and are discussed individually below.

*Aluminum.* The resultant spectrum for aluminum is shown in Fig. 2. The data seem to suggest an exponential dependence on energy, and a fit of the data points (excepting the 39-MeV point, which may be subject to threshold problems) to an exponential  $e^{-E/E_0}$  yields  $E_0 = 7.5 \pm 0.4$  MeV. The integrated intensity above 40 MeV is  $(1.38 \pm 0.09) \times 10^{-3}$  per captured muon. The total probability<sup>14</sup> for reactions of the form  $(\mu^-, pxn)$ ,  $(\mu^-, 2pn)$ , and  $(\mu^-, \alpha)$  is of order  $10^{-1}$ , indicating that high-energy charged particles are emitted in approximately 2% of the capture events.

No previous results have been reported for alum-

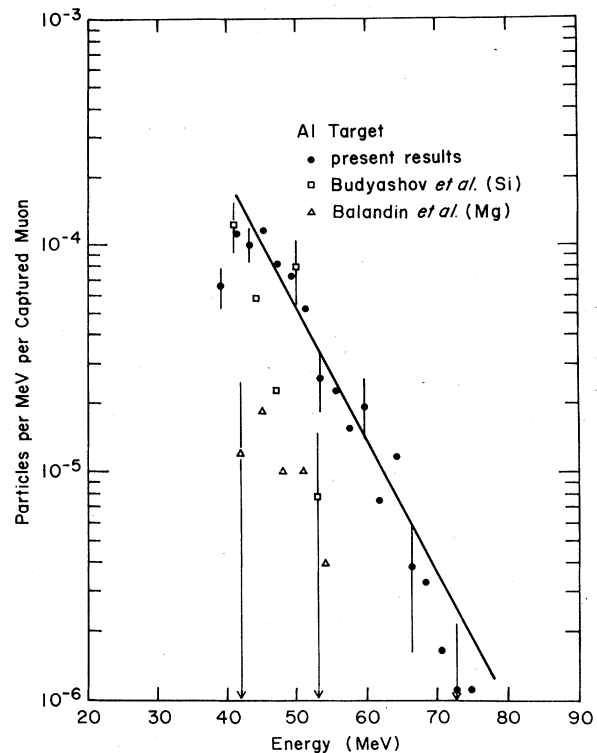


FIG. 2. Yield of charged particles following  $\mu^-$  capture in aluminum target. The filled circles represent results of the present work, with representative error bars shown. The straight line is an exponential fit to the data with  $E > 40$  MeV. The open squares represent results of Budyashov *et al.* (Ref. 12) for silicon. The open triangles represent results of Balandin *et al.* (Ref. 13) for magnesium.

inum, but spectra have been measured for neighboring elements by Budyashov *et al.*<sup>12</sup> (silicon) and by Balandin *et al.*<sup>13</sup> (magnesium). Their results for the yield above 40 MeV are, respectively,  $(0.87 \pm 0.14) \times 10^{-3}$  for silicon and  $(0.17 \pm 0.05) \times 10^{-3}$  for magnesium. Both the integrated yield and the energy dependence (shown in Fig. 2) for silicon are in reasonable agreement with those of the present work for Al, while magnesium shows considerably less intensity than aluminum. This suggests the possibility of an interesting dependence on nuclear structure in this mass range.

**Copper.** Figure 3 illustrates the present results for the copper target. As above, the data for  $E > 40$  MeV suggest an exponential dependence of the yield on the particle energy, with  $E_0 = 8.3 \pm 0.5$  MeV. The integrated yield for energies above 40 MeV is  $(1.96 \pm 0.12) \times 10^{-3}$  per captured muon. The total yield (for all charged-particle final states) from activation studies<sup>14</sup> is of order  $4 \times 10^{-2}$ , so that the high-energy yield constitutes about 5% of the charged-particle emission following  $\mu$ -capture. Previous work by Budyashov *et al.*<sup>12</sup> is also shown in Fig. 3; their integrated yield (protons plus deuterons) above 40 MeV is  $(0.67 \pm 0.19) \times 10^{-3}$ , about

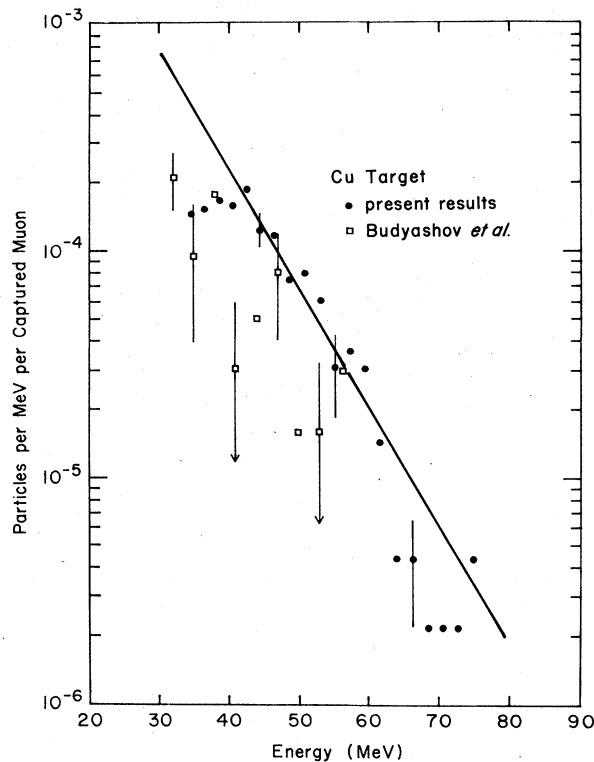


FIG. 3. Yield of charged particles following  $\mu^-$  capture in copper target. The straight line is the result of an exponential fit to the data above 40 MeV. The open squares represent data of Budyashov *et al.* (Ref. 12).

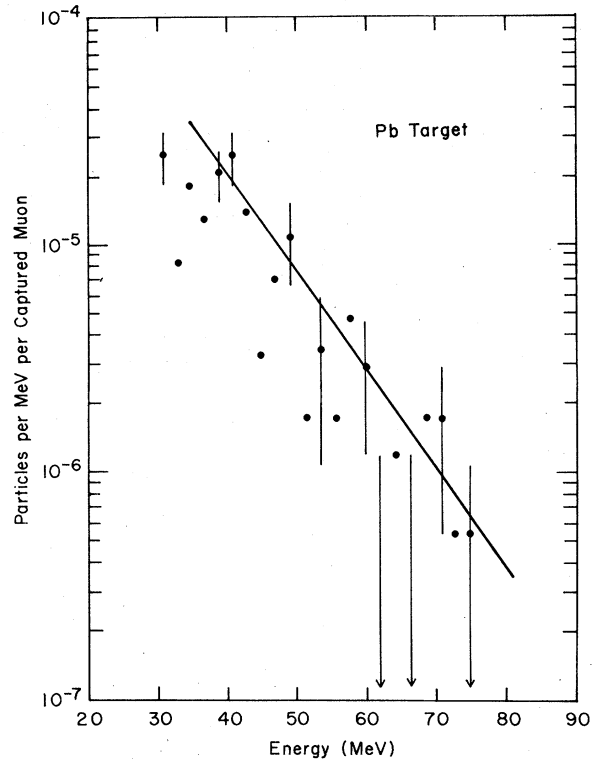


FIG. 4. Yield of charged particles following  $\mu^-$  capture in lead target. The straight line is an exponential fit to the data with  $E > 40$  MeV.

a factor of 3 smaller than our result.

**Lead.** The results obtained with the Pb target are shown in Fig. 4. The slope of the fitted line yields  $E_0 = 9.9 \pm 1.1$  MeV, and the integrated yield for  $E > 40$  MeV is  $(1.71 \pm 0.28) \times 10^{-4}$  per captured muon; this yield is about an order of magnitude smaller than that obtained with the Al and Cu targets and represents about 4% of the total charged-particle yield as determined in activation studies.<sup>14</sup> These results are summarized in Table I.

#### IV. DISCUSSION

The theoretical situation relating to the interpretation of energetic particles emitted following

TABLE I. Charged-particle yield following  $\mu^-$  capture.

Target	$E_0^a$ (MeV)	Integrated yield $E > 40$ MeV ( $\times 10^3$ )
Al	$7.5 \pm 0.4$	$1.38 \pm 0.09$
Cu	$8.3 \pm 0.5$	$1.96 \pm 0.12$
Pb	$9.9 \pm 1.1$	$0.171 \pm 0.028$

<sup>a</sup> Exponential constant, assuming yield  $\propto \exp(-E/E_0)$ .

muon capture has been reviewed by Singer.<sup>1</sup> The lack of structure in the observed high-energy particle spectrum makes difficult a comparison among competing theoretical models, but a common feature of the spectra recorded in the present work is the roughly exponential nature of the particle spectrum. The neutron spectra<sup>1</sup> observed following muon capture are similarly structureless and exponential. This similarity may be more than coincidental, since in one interpretation the outgoing proton results from charge exchange by the outgoing primary neutron emitted in  $\mu$  capture. The resultant proton spectrum can then be obtained by modifying the neutron spectrum by the probability for such ( $n, p$ ) charge exchange reactions.<sup>18</sup> It is therefore instructive to compare the exponential constants of the measured neutron spectra with those of the proton spectra. No neutron data are available for Al, but the neutron spectrum from neighboring Si has been measured by Sundelin and Edelstein,<sup>19</sup> who find  $E_0 = 7.6$  MeV. Neutron spectra for Pb have been obtained by Krieger<sup>20</sup> ( $E_0 = 12 \pm 1$  MeV) and by Schröder *et al.*<sup>21</sup> ( $E_0 = 9.0 \pm 1.2$ ). (However, it must be noted that

the various neutron results are not in good mutual agreement; for Ca, Sundelin and Edelstein give  $E_0 = 7.2$ , Krieger gives  $E_0 = 14 \pm 1$ , while Schröder *et al.* give  $E_0 = 8.4 \pm 1.0$ .) Thus the expectation that the proton spectrum shows a steeper exponential falloff than the neutron spectrum seems not to be supported by our results, which indicate that the proton and neutron spectra show similar energy dependence.

Although our results do not enable one to distinguish from among the competing theoretical explanations for charged-particle emission, we have verified the surprisingly large number of high-energy particles emitted following  $\mu^-$  capture.

#### ACKNOWLEDGMENTS

We are pleased to acknowledge the suggestion of Dr. C. Werntz regarding the comparison of proton and neutron spectra to elicit information on charge exchange. This work was supported in part by the National Science Foundation and by the U. S. Department of Energy.

<sup>1</sup>See, for example, the review by P. Singer, Springer Tracts Mod. Phys. **71**, 39 (1974).

<sup>2</sup>Yu. A. Batusov and R. A. Eramzhyan, Fiz. Elem. Chastits At. Yadra **8**, 229 (1977) [Sov. J. Part. Nucl. **8**, 95 (1977)].

<sup>3</sup>H. Morinaga and W. F. Fry, Nuovo Cimento **10**, 308 (1953).

<sup>4</sup>C. Ishii, Prog. Theor. Phys. **21**, 663 (1959).

<sup>5</sup>P. Singer, Phys. Rev. **124**, 1602 (1961).

<sup>6</sup>M. Bertero, G. Passatore, and G. A. Viano, Nuovo Cimento **38**, 1669 (1965).

<sup>7</sup>H. Uberall, Phys. Rev. **139**, B1239 (1965).

<sup>8</sup>J. Bernabéu, T. E. O. Ericson, and C. Jarlskog, Phys. Lett. **69B**, 161 (1977).

<sup>9</sup>D. Kotelchuck and J. V. Tyler, Phys. Rev. **165**, 1190 (1968).

<sup>10</sup>S. E. Sobottka and E. L. Wills, Phys. Rev. Lett. **20**, 569 (1968).

<sup>11</sup>A. O. Vaisenberg, E. D. Kolganove, and N. V. Rabin, Yad. Fiz. **11**, 830 (1970) [Sov. J. Nucl. Phys. **11**, 464 (1970)].

<sup>12</sup>Yu. G. Budyashov, V. G. Zinov, A. D. Konin, A. I. Muk-

hin, and A. M. Chatrchyan, Zh. Eksp. Teor. Fiz. **60**, 19 (1971) [Sov. Phys.-JETP **33**, 11 (1971)].

<sup>13</sup>M. P. Balandin, V. M. Grebeniuk, V. G. Zinov, T. Kozlovski, and A. D. Konin, JINR Report No. P15-11215, Dubna, 1978 (unpublished).

<sup>14</sup>A. Wytttenbach, P. Baertschi, S. Bajo, J. Hadernann, K. Junken, S. Katcoff, E. A. Hermes, and H. S. Pruys, Nucl. Phys. **A294**, 278 (1978).

<sup>15</sup>M. Lifshitz and P. Singer, Phys. Rev. Lett. **41**, 18 (1978).

<sup>16</sup>See, for example, P. Singer, N. C. Mukhopadhyay, and R. D. Amado, Phys. Rev. Lett. **42**, 162 (1979).

<sup>17</sup>J. C. Sens, Phys. Rev. **113**, 679 (1959).

<sup>18</sup>M. Sternheim and R. R. Silbar, Phys. Rev. Lett. **34**, 824 (1975).

<sup>19</sup>R. M. Sundelin and R. M. Edelstein, Phys. Rev. C **7**, 1037 (1973).

<sup>20</sup>M. H. Krieger, thesis, Columbia University, 1969 (unpublished). See also Ref. 1.

<sup>21</sup>W. O. Schröder, U. Jahnke, K. H. Lindenberger, G. Röschert, R. Engfer, and H. K. Walter, Z. Phys. **268**, 57 (1974).